Int. J. Electrochem. Sci., 8 **(2013)** 9558 - 9567

International Journal of
ELECTROCHEMICAL
SCIENCE
www.electrochemsci.org

Ether-Functionalized Pyrazolium Ionic Liquids as Electrolytes for Dye Sensitized Solar Cells

Yizhou Zheng[1], *Qiyu Huang*[1,*], *Shaohua Fang*[2], *Li Yang*[2,*], *Yuchou Gan*[1]

[1]School of Microelectronics, Shanghai Jiao Tong University, Shanghai 200240, P. R. China
[2]School of Chemistry and Chemical Engineering, Shanghai Jiao Tong University, Shanghai 200240, P. R. China
[*]E-mail: qiyu@sjtu.edu.cn; liyangce@sjtu.edu.cn

Received: 9 May 2013 / *Accepted:* 9 June 2013 / *Published:* 1 July 2013

Two ether-functionalized ionic liquids (ILs) based on pyrazolium cations and bis(trifluoromethylsulfonyl)imide anions ($TFSI^-$) as solvent and pyrazolium iodide as iodide source were first time fabricated for dye sensitized solar cells (DSSCs). The I-V characteristic curves, electrochemical impedance spectroscopy (EIS) and linear sweep voltammetry (LSV) demonstrated the performance of functionalized ILs as well as the performance of dye sensitized solar cells with the change of the concentration of iodide and iodine. It was confirmed by EIS that mass-transport limitation becoming less of a problem in the 1-(2-Methoxyethyl)-2-ethylpyrazolium (OEPZ)-based and 1-(2-Methoxyethyl)-2-methylpyrazolium (OMPZ)-based electrolytes. A maximum of 1.7% efficiency was obtained with the observed photo-voltage of 0.557V and photocurrent density of 6.3mA/cm^2 using the electrolyte concentration of 0.1M I_2 and 1M OEPZ-iodide in OEPZ-TFSI for fabrication of the solar cell without additives at 100mW/cm^2. The DSSC based on OMPZ electrolyte exhibited lower efficiency due to large resistances.

Keywords: ionic liquids, functionalized cations, dye sensitized solar cell (DSSC)

1. INTRODUCTION

Dye sensitized solar cells are attracting more and more attention due to their relative high energy conversion efficiency, low cost and environmental friendliness. Using a volatile electrolyte (i.e. acetonitrile solvent), an efficiency record of over 11% has been achieved among all types of organic photovoltaic cells [1-3]. However, the use of volatile electrolytes caused degradation of performance of DSSCs by introducing problems such as liquids evaporation at high temperature and permeation of water and oxygen molecules into the electrolyte. These problems limited their large-scale

implementation due to poor long-term stability and the necessity for a complex sealing process [4-6]. Therefore, using non-volatile electrolytes like room-temperature ionic liquids (RTIL) [7, 8] and solid-state hole-transporting materials are the solutions to the problem mentioned previously. RTILs are the promising alternatives to volatile electrolytes due to their unique properties, such as negligible vapor pressure, excellent electrochemical and thermal stability, as well as high ionic conductivity [9-11].

Pyrazolium cation has similar C-N heterocyclic structure with imidazolium cation except the positions of the two N atoms [12]. However, researches in pyrazolium are less compared with imidazolium. Abu-Lebdeh group [13, 14] synthesized a series of ILs based on pyrazolium cations and $TFSI^-$. These ILs were applied as electrolytes in $Li_4Ti_5O_{12}/LiFePO_4$ cells [15, 16]. 1-Methyl-2-ethylpyrazolium BF_4 ($EMPBF_4$) [17] and three 1-alkyl-2,3,5-trimethylpyrazolium ILs [18] had been reported to be used in $MoO_2/LiMn_2O_4$ and lithium batteries respectively. A series of 1-alkyl-2-methylpyrazolim iodide ILs were applied in DSSCs. This was the only one paper reporting pyrazolium based ILs used in DSSCs [19]. Also some pyrazolium ILs had been investigated as catalysts [20] and antibacterial cationic surfactants [21].

High melting point is one of the main problems limiting the wide applications of prazolium ILs in electrochemical devices. Ether group was an electron-donating group which could weaken the electrostatic interaction between cation and anion, and thus resulted in reducing the melting points and viscosities of ILs without causing obvious degradation of electrochemical stability of ILs [22, 23]. Recently, L. Yang group [12] synthesized four new pyrazolium ILs with ether group, which showed the properties of low viscosity and low melting point. Especially the viscosity of OEPZ-TFSI was 41.2mPa•s at 25℃, which was the lowest value among the pyrazolium ILs reported [18].

We hereby used two pyrazolium ILs with low viscosity, OEPZ-TFSI and OMPZ-TFSI, as solvents and corresponding pyrazolium based iodide with ether group as an iodide source for fabrication of dye sensitized solar cells. OEPZ and OMPZ cations were used for the first time in the electrolytes in DSSCs. The electrochemical methods, such as EIS and LSV, were used to characterize pyrazolium based electrolytes for DSSCs.

2. EXPERIMENTAL

2.1. Materials

All solvents and reagents, unless otherwise stated, were of analytical quality and used as received. And commercially available materials were purchased from Heptachroma Ltd. and Casjuxin Solar Technology Ltd.. OEPZ-TFSI, OEPZI, OMPZ-TFSI and OMPZI were all homemade. Conducting glass plates (F: SnO_2 conducting glass with sheet resistance of 15ohm/□) were used as substrate for screen printing of TiO_2 porous films.

2.2. Fabrication of photovoltaic devices

Nanocrystalline TiO_2 film was coated on FTO conducting glass substrate by screen printing technique and annealed at 450℃ for 30min. The TiO_2 coated glass plate was then stained by dipping it

in a 0.3mM anhydrous ethanol solution of N719 dye at room temperature for 24h. Afterwards, the electrode was withdrawn from the solution and dried. A platinized counter electrode and photo- anode electrode were sandwiched by a 45μm thick Surlyn hot-melt ring. The internal space was filled with ionic liquids.

2.3. Measurements

The current-voltage characteristics of the solar cells were measured with a Keithley 2400 digital source meter by applying an external bias voltage to the cell under xenon lamp of intensity 100mW/cm^2. The EIS and LSV were both obtained with CHI660D electrochemical workstation in the dark condition. The EIS was obtained in the frequency range of 0.01Hz to 0.1MHz with an AC amplitude of 5mV. The apparent diffusion coefficient of I_3^- was measured by a method described in the literature [24]. The symmetric electrochemical cells composed of two conventional platinized conducting electrodes separated by Surlyn of 45μm were used. The applied voltage was swept from -0.8V to 0.8V with the slow scan rate of 10mV/s.

3. RESULTS AND DISCUSSION

3.1. Influence of iodide source concentration on the performance of DSSCs

Figure 1 showed the dependence of short-circuit current density (J_{sc}) and power-conversion efficiency (η) on the concentration of iodide. The curves in Fig. 1 were based on six different blends. They were OEPZ-TFSI and OMPZ-TFSI with varying iodide concentration of 0.8M, 1M and 1.2M, while the concentration of iodine was fixed to be 0.1M. For OEPZ-based electrolytes, J_{sc} andηwere increased first when the concentration of OEPZ-I in OEPZ-TFSI was raised from 0.6M to 1M. The J_{sc} andηvalues were decreased with the further increase of the OEPZ-I concentration.

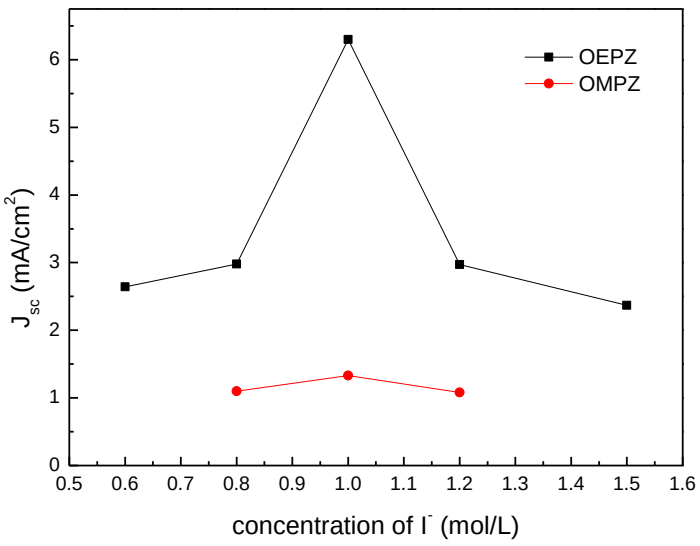

A

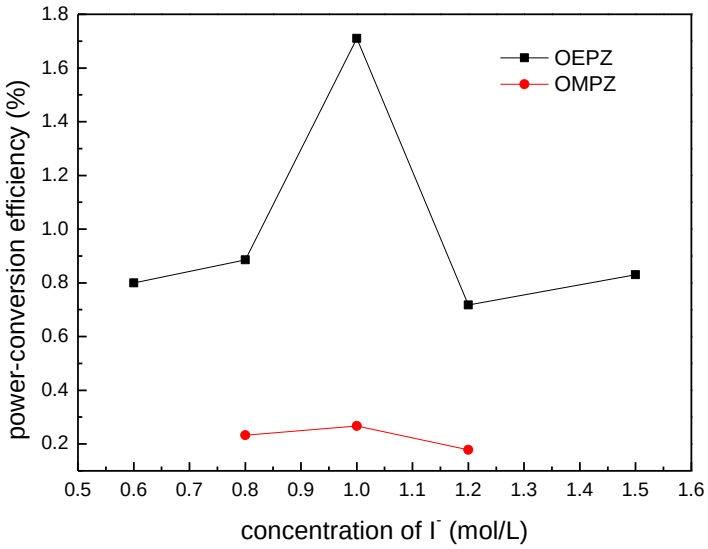

B

Figure 1. Dependence of (a) photocurrent density and (b) power conversion efficiency of devices on the concentration of iodide under AM1.5 full sunlight

Table 1. Photovoltaic parameters of DSSCs at varying iodide concentration, ranging from 0.6 to 1.5M, including short-circuit current densities (J_{sc}), open-circuit voltage (V_{oc}), fill factor (FF) and power conversion efficiencies (η).

Iodide concentration(M)	J_{sc} (mA/cm^2)		V_{oc} (v)		FF		E_{FF} (%)	
	OEPZ	OMPZ	OEPZ	OMPZ	OEPZ	OMPZ	OEPZ	OMPZ
0.8	2.98	1.10	0.56	0.423	0.53	0.5	0.885	0.23
1	6.30	1.33	0.557	0.420	0.48	0.477	1.7	0.267
1.2	2.97	1.08	0.55	0.371	0.439	0.445	0.718	0.178

As the concentration of iodide increased, the concentration of I^- increased, giving faster dye regeneration for further photon-induced electron generation and injection, and thus an increase in J_{sc} andη. Nevertheless, too high of an I^- concentration not only increased the combination probability between the conduction band electrons and I_3^- , causing a decrease in J_{sc}, but also resulted in high viscosity which was observed later on. The largest J_{sc} of OEPZ was 6.3 mA/cm^2 and the efficiency achieved was 1.7% at the OEPZ-I concentration of 1M. The same trend could be observed when using OMPZ- based electrolytes. However, both the J_{sc} and FF, influenced by the ionic conductivity of ILs, were much lower than OEPZ based ILs, because OMPZ-TFSI had higher viscosity than OEPZ-TFSI's [12]. Low conductivity caused large series resistance [25] and it was directly affected by viscosity and diffusion coefficient of the electrolyte. A complete set of photovoltaic parameters for different concentration of OEPZI was shown in Table 1.

3.2. Correlation between the I_2 concentration and the I_3^- diffusion coefficient

According to the above mentioned experiment, I^- concentrations of OEPZ-I and OMPZ-I were kept at 1M. The influence of the I_2 concentration in the OEPZ/OMPZ-based electrolytes was researched by evaluating the mass transport in the DSSCs. A symmetrical thin-layer dummy cell was used for the measurement of limiting current densities, which was consisted of two platinized counter electrodes. It was assumed that I^- and I_2 immediately formed I_3^- in the liquid. The apparent diffusion coefficient of triiodide was measured as described in the measurement section as a function of concentration of iodine.

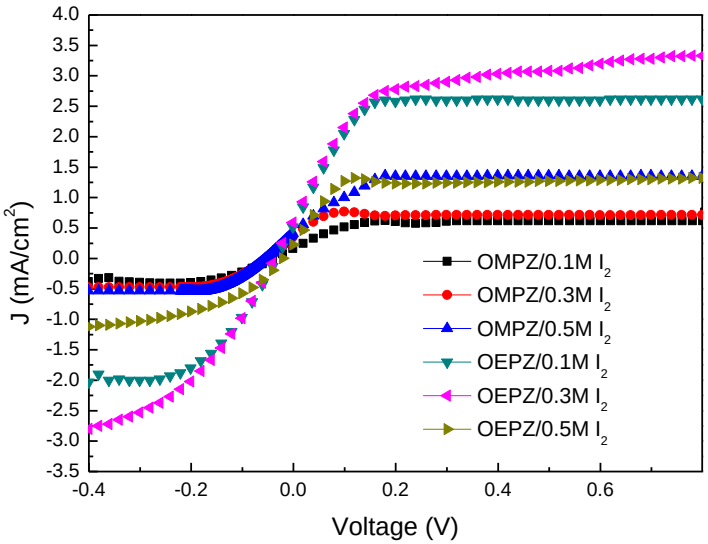

Figure 2. Linear sweep voltammograms of ionic liquids at varying concentration of I_2 (0.1M to 0.5M).

The limiting current densities of the electrolytes containing various concentration of iodine were illustrated in Fig. 2 OEPZ-based electrolyte containing 0.3M I_2 had largest limiting current density of 3.33 mA/cm^2, followed by the electrolyte containing 0.1M I_2, which was 2.62 mA/cm^2. The maximum limiting current density of OMPZ-based electrolytes was 1.36mA/cm^2 which was approximately three times lower than that of the OEPZ-based. The apparent diffusion coefficient (D_{app}) of triiodides can be calculated from the limiting current densities according to the equation,

$$J_{\lim} = 2nFC_0D_{app} / d \qquad (1)$$

where n is the electron-transfer number required for the reduction of triiodide to iodide, F the Faraday constant, C_0 the bulk concentration of triiodide ions and d the thickness of the cell. The correlation between I_2 concentration and I_3^- diffusion coefficient was summarized in Table 2. The highest apparent diffusion coefficient of triiodide ($3.05*10^{-7}$cm^2/s) was observed in the OEPZ/0.1M I_2. In contrast, the lowest apparent diffusion coefficient of triiodide ($0.277*10^{-7}$cm^2/s) was found in the OMPZ/0.3M I_2. The triiodide diffusion coefficient of the OEPZ- and OMPZ-based electrolytes decreased in the following order: OEPZ/0.1M I_2 > OEPZ/0.3M I_2 > OMPZ/0.1M I_2 >OEPZ/0.5M I_2 > OMPZ/0.5M I_2 > OMPZ/0.3M I_2. This order implied that the mass-transport limitation became less of a problem in the OEPZ- and OMPZ-based electrolytes [4, 26]. But it was against the common

knowledge that the relatively high viscosities of ionic liquids require higher iodine concentration in the electrolyte due to mass-transport limitations of the triiodide ions.

Table 2. Limiting current density (J_{lim}) and apparent diffusion coefficient of triiodide (D_{app}) in the ILs at different iodine concentration.

Iodine Concentration	J_{lim} (mA/cm^2)		I_3^- D_{app} (10^{-7}cm^2/s)	
	OEPZ	OMPZ	OEPZ	OMPZ
0.1M	2.62	0.619	3.05	0.72
0.3M	3.33	0.714	1.295	0.277
0.5M	1.32	1.36	0.308	0.317

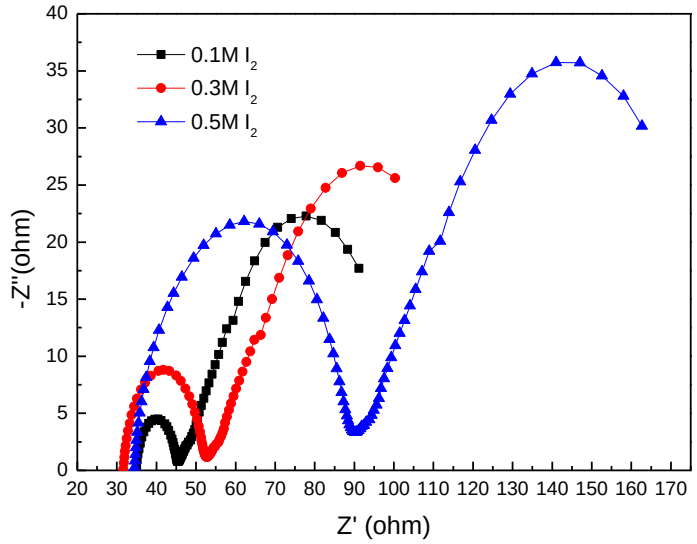

A

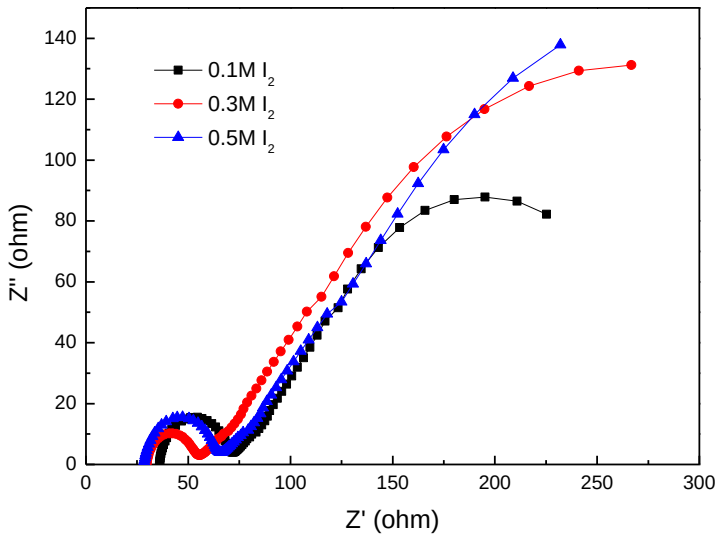

B

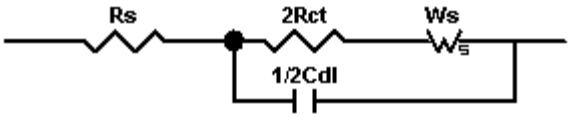

C

Figure 3. Nyquist plots of (a) OEPZ-based devices and (b) OMPZ-based devices with different iodine concentration ILs measured in the dark. (c) Randles equivalent circuit including components of R_s = series resistance, R_{ct} = charge transfer resistance, C_{dl} = double layer capacitance, and W_s = Warburg impedance.

Table 3. Fitted resistances of symmetrical cells with different iodine concentration ILs from the EIS measurements.

Iodine Concentration	$R_s(\Omega cm^2)$		$R_{ct}(\Omega cm^2)$		$W_s(\Omega cm^2)$	
	OEPZ	OMPZ	OEPZ	OMPZ	OEPZ	OMPZ
0.1M	21.15	20.18	2.92	8.84	32.23	125.89
0.3M	19.42	16.69	5.69	6.33	45.81	167.04
0.5M	21.56	16.17	13.92	9.17	111.78	186.07

To clarify this discrepancy, EIS measurements were used to investigate the electronic transport in the electrolytes and the charge transfer reaction at the interface. Figure 3 showed the corresponding Nyquist spectra of the symmetrical thin-layer cells with different electrolytes containing different concentration of iodine. Generally, the spectrum consists of a semicircle in the high-frequency region relates to the charge transfer at the counter electrode, and a semicircle in the low-frequency region relates to the Warburg diffusion processes in the electrolyte.

Resistance parameters were fitted with the Randles equivalent circuit [27] shown in Fig. 3(c) and Zview software. Resistance parameters summarized in Table 3 demonstrated the mechanism for electron transport. The series resistance, the Warburg diffusion resistance and the charge transfer resistance at the counter electrode were dependent on the viscosities of electrolytes. Among the OEPZ/OMPZ-based ILs, the one with 0.1M iodine had the lowest resistances, with R_s, R_{ct} and W_s were 21.15Ωcm^2, 2.92Ωcm^2 and 32.23Ωcm^2 respectively. And conversely, the electrolyte with 0.5M iodine exhibited the highest R_{ct} and W_s. The W_s decreased in the following order: OMPZ/0.5M I_2 > OMPZ/0.3M I_2 > OMPZ/0.1M I_2 > OEPZ/0.5M I_2 > OEPZ/0.3M I_2 > OEPZ/0.1M I_2. It approximately coincided with the trend of the triiodide diffusion coefficient. Therefore, an increase in concentration of iodine not only slowed down the charge transfer process at the counter electrode but also decreased the diffusion coefficient of triiodide ascribed to large diffusion resistance. While the mass-transport limitation had less influence in OEPZ/OMPZ-based electrolytes, a lower iodine concentration was more favorable. This eliminated the negative effects of high viscosity and the extra electron recombination deriving from the additional iodine in the electrolytes.

3.3. The performance of DSSCs based on OEPZ and OMPZ electrolytes

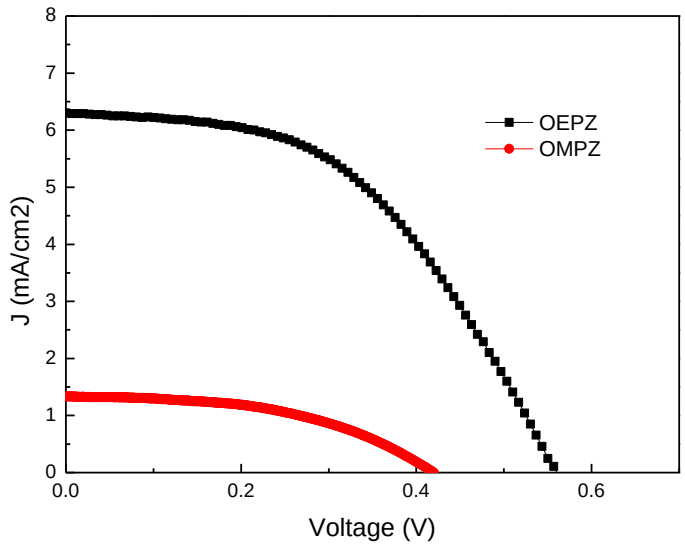

Figure 4. Photocurrent density-voltage curves for DSSCs using OEPZ- and OMPZ-based electrolytes with 0.1M iodine and 1M iodide.

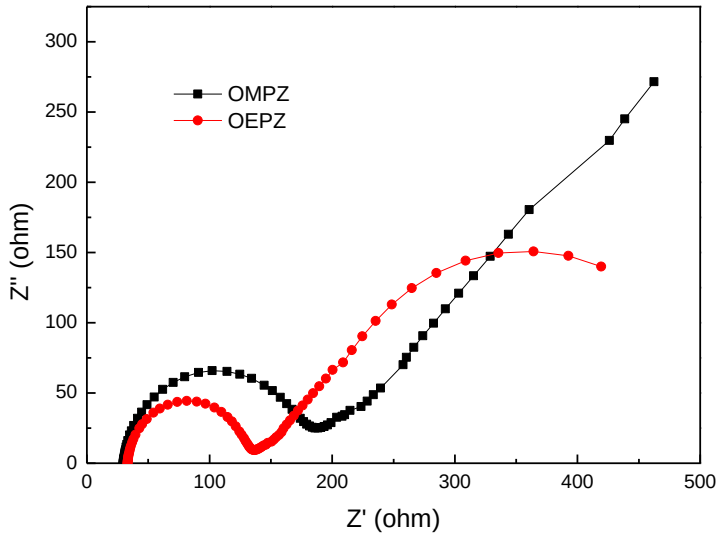

Figure 5. Impedance spectra of DSSCs containing OEPZ- and OMPZ-based electrolytes with 0.1M iodine and 1M iodide obtained at a bias voltage of -0.55V in the dark.

Figure 4 showed the photocurrent density-voltage curves for DSSCs using OEPZ- and OMPZ-based electrolytes with 0.1M iodine and 1M iodide. Comparing these two electrolytes, DSSC with OEPZ-based electrolyte had higher V_{oc} and J_{sc}. V_{oc} is determined by the conduction band of TiO_2 (CB) and the electron lifetimes in the CB [26]. Since there were no additives in these two electrolytes, the difference can be ascribed to the electron lifetimes in the CB of TiO_2. This assumption could be proved by EIS, as shown in Fig. 5 The recombination resistance at the TiO_2/electrolyte interface (the second semicircle) for the OEPZ-based electrolyte was lower compared to that of OMPZ-based, and thus less

electron recombination occurred at the TiO_2/OEPZ-based electrolyte interface. Therefore, longer electron lifetimes contributed to higher V_{oc}. J_{sc} is determined by viscosity of electrolyte, which had been discussed in section 3.1. The highest power conversion efficiency of DSSC with OEPZ-based electrolyte reached 1.7% without additives, which was better than that of OMPZ-based.

4. CONCLUSION

In summary, two pyrazolium with ether group based ionic liquids as electrolytes were used and their electrochemical properties were investigated for their potential application in dye sensitized solar cells. LSV and EIS measurements indicated that the performance of prazolium based ILs had dramatic dependence on its viscosity with different concentrations of iodine and iodide. Especially the apparent diffusion of triiodide decreased with the variation of the concentration of iodine from 0.1M to 0.5M. It demonstrated that the mass-transport limitation had less influence in OEPZ/OMPZ-based electrolytes and a lower iodine concentration was more favorable. With 0.1M iodine and 1M iodide concentration, the highest power conversion efficiency reached 1.7% without additives.

ACKNOWLEDGEMENTS
This work was supported by the Shanghai Minhang Science and Technology Committee District-University Collaboration Program under Grant #2011MH060. The authors would like to thank and acknowledge the assistance of the staff and students of the Shanghai Jiao Tong University Microfabrication Laboratory.

References

1. J.M. Kroon, N.J. Bakker, H.J.P. Smit, P. Liska, K.R. Thampi, P. Wang, S.M. Zakeeruddin, M. Gratzel, A. Hinsch, S. Hore, U. Wurfel, R. Sastrawan, J.R. Durrant, E. Palomares, H. Pettersson, T. Gruszecki, J. Walter, K. Skupien and G.E. Tulloch, *Prog. Photovoltaics*, 15 (2007) 1
2. M.K. Nazeeruddin, F. De Angelis, S. Fantacci, A. Selloni, G. Viscardi, P. Liska, S. Ito, T. Bessho and M. Gratzel, *J. Am. Chem. Soc.*, 127 (2005) 16835
3. Y. Chiba, A. Islam, R. Komiya, N. Koide and L.Y. Han, *Appl. Phys. Lett.*, 88 (2006)
4. N. Papageorgiou, Y. Athanassov, M. Armand, P. Bonho, H. Pettersson, A. Azam and M. Grätzel, *J. Electrochem. Soc.*, 143 (1996) 3099
5. A. Hinsch, J. Kroon, R. Kern, I. Uhlendorf, J. Holzbock, A. Meyer and J. Ferber, *Prog. Photovoltaics*, 9 (2001) 425
6. P.-Y. Chen, C.-P. Lee, R. Vittal and K.-C. Ho, *J. Power Sources*, 195 (2010) 3933
7. P.N. Tshibangu, S.N. Ndwandwe and E.D. Dikio, *Int. J. Electrochem. Sci.*, 6 (2011) 2201
8. B. Baek, S. Lee and C. Jung, *Int. J. Electrochem. Sci.*, 6 (2011) 6220
9. R. Kawano and M. Watanabe, *Chem. Commun.*, (2005) 2107
10. P. Wang, S.M. Zakeeruddin, P. Comte, I. Exnar and M. Grätzel, *J. Am. Chem. Soc.*, 125 (2003) 1166
11. D. Kuang, P. Wang, S. Ito, S.M. Zakeeruddin and M. Grätzel, *J. Am. Chem. Soc.*, 128 (2006) 7732
12. M. Chai, Y.D. Jin, S.H. Fang, L. Yang, S. Hirano and K. Tachibana, *J. Power Sources*, 216 (2012) 323
13. Y. Abu-Lebdeh, P.J. Alarco and M. Armand, *Angew. Chem. Int. Ed.*, 42 (2003) 4499

14. P.-J. Alarco, Y. Abu-Lebdeh, N. Ravet and M. Armand, *Solid State Ionics*, 172 (2004) 53
15. P.-J. Alarco, Y. Abu-Lebdeh and M. Armand, *Solid State Ionics*, 175 (2004) 717
16. Y. Abu-Lebdeh, A. Abouimrane, P.-J. Alarco and M. Armand, *J. Power Sources*, 154 (2006) 255
17. J. Čaja, T.D.J. Dunstan, H.A. Dyar, H. Krall and V. Katović, *Kem. Ind.*, 54 (2005) 205
18. S. Seki, T. Kobayashi, N. Serizawa, Y. Kobayashi, K. Takei, H. Miyashiro, K. Hayamizu, S. Tsuzuki, T. Mitsugi and Y. Umebayashi, *J. Power Sources*, 195 (2010) 6207
19. N. Ishimaru, W. Kubo, T. Kitamura, S. Yanagida, Y. Tsukahara, M.M. Maitani and Y. Wada, *Mater. Sci. Eng., B*, 176 (2011) 996
20. Y. Han, H.V. Huynh and G.K. Tan, *Organometallics*, 26 (2007) 6581
21. N.A. Negm, M.M. Said and S.M. Morsy, *J. Surfactants Deterg.*, 13 (2010) 521
22. M. Chai, Y. Jin, S. Fang, L. Yang, S.-i. Hirano and K. Tachibana, *Electrochim. Acta*, 66 (2012) 67
23. S. Fang, Z. Zhang, Y. Jin, L. Yang, S.-i. Hirano, K. Tachibana and S. Katayama, *J. Power Sources*, 196 (2011) 5637
24. N. Papageorgiou, W. Maier and M. Grätzel, *J. Electrochem. Soc.*, 144 (1997) 876
25. R. Kern, R. Sastrawan, J. Ferber, R. Stangl and J. Luther, *Electrochim. Acta*, 47 (2002) 4213
26. Z. Yu, N. Vlachopoulos, A. Hagfeldt and L. Kloo, *Rsc Adv.*, 3 (2013) 1896
27. F. Hao, H. Lin, Y.Z. Liu and J.B. Li, *Phys. Chem. Chem. Phys.*, 13 (2011) 6416